

# New Synthetic Route to (3-Glycidoxypropyl)trimethoxysilane-Based Hybrid Organic–Inorganic Materials

Plinio Innocenzi,<sup>\*,†</sup> Giovanna Brusatin,<sup>†</sup> Massimo Guglielmi,<sup>†</sup> and  
Roberta Bertani<sup>‡</sup>

*Dipartimento di Ingegneria Meccanica, Settore Materiali, Università di Padova,  
via Marzolo 9, 35131 Padova, Italy, and Centro di Chimica Metallorganica del CNR,  
Dipartimento Processi Chimici dell'Ingegneria, Facoltà di Ingegneria, Università di Padova,  
via Marzolo 9, 35131 Padova, Italy*

*Received July 20, 1998. Revised Manuscript Received March 30, 1999*

Hybrid organic–inorganic materials have been obtained by cohydrolysis of (3-glycidoxypropyl)trimethoxysilane (GPTMS) and tetraethyl orthosilicate (TEOS) in acidic conditions. Boron trifluoride diethyl etherate (BF<sub>3</sub>OEt<sub>2</sub>) has been used to catalyze the epoxide polymerization. The effect of BF<sub>3</sub>OEt<sub>2</sub> has been studied by multinuclear magnetic resonance (NMR) in the precursor sol and by Fourier transform infrared spectroscopy in the final material. The addition of BF<sub>3</sub>OEt<sub>2</sub> to a prereacted sol of GPTMS and TEOS has allowed the epoxide ring opening at room temperature, without formation of diol units or boric acid precipitation in the final material. The prereaction time of GPTMS with TEOS has been found to be an important parameter. The catalytic effect of BF<sub>3</sub>OEt<sub>2</sub> with respect to other commonly used catalysts in sol–gel processing of GPTMS-based hybrid organic–inorganic materials, such as zirconium butoxide and 1-methylimidazole, has been studied.

## Introduction

Organic–inorganic hybrid materials based on (3-glycidoxypropyl)trimethoxysilane (GPTMS) have several important applications, such as antiscratch coatings,<sup>1</sup> contact lens materials,<sup>2</sup> passivation layers for microelectronics,<sup>3</sup> multifunctional coatings,<sup>4</sup> and optical devices.<sup>5–7</sup> GPTMS-derived optical waveguides, in particular, are a very promising material because of the possibility to incorporate optically active organic molecules in a matrix that is dense at low temperature and with a high degree of microstructural homogeneity.<sup>8,9</sup>

GPTMS is an organically modified alkoxide, whose organic group contains an epoxide ring that can be cross-linked to form a poly(ethylene oxide) chain and acts, therefore, as network former. The use of GPTMS in sol–gel processing allows a material to be obtained with higher density at low temperatures (100–150 °C) than in the case of organically modified alkoxides whose

organic groups are, instead, network modifiers, such as, for instance, CH<sub>3</sub>Si(OC<sub>2</sub>H<sub>5</sub>)<sub>3</sub> and C<sub>6</sub>H<sub>5</sub>Si(OC<sub>2</sub>H<sub>5</sub>)<sub>3</sub>.<sup>10</sup>

GPTMS-based sol–gel reactions were the subject of several specific studies by nuclear magnetic resonance (NMR),<sup>11–15</sup> Raman spectroscopy,<sup>16,17</sup> and gel permeation chromatography.<sup>18</sup> The ring opening of GPTMS epoxides is usually achieved, in the synthesis of sol–gel hybrid organic–inorganic materials, by titanium or zirconium alkoxides,<sup>15,19,20</sup> whose use has, however, some disadvantages because of their high reactivity and the necessity of using a chelating agent to reduce their hydrolysis rate. The chelating agents (for instance, 2,4-pentanedione or acetic acid), because of the low temperatures of curing required by the process, remain in the microstructure and modify the optical properties, such as the optical losses in waveguides. The change in the refractive index and optical absorption of the material with the introduction of zirconia and titania in the

<sup>†</sup> Dipartimento di Ingegneria Meccanica.

<sup>‡</sup> Centro di Chimica Metallorganica del CNR.

(1) Nass, R.; Arpac, E.; Glaubitt, W.; Schmidt, H. *J. Non-Cryst. Solids* **1990**, *121*, 370.

(2) Philipp, G.; Schmidt, H. *J. Non-Cryst. Solids* **1984**, *63*, 283.

(3) Popall, M.; Kappel, J.; Pilz, M.; Schulz, J.; Feyder, G. *J. Sol-Gel Sci. Technol.* **1994**, *2*, 157.

(4) Schmidt, H. *J. Non-Cryst. Solids* **1994**, *178*, 302.

(5) Sorek, Y.; Reisfeld, R.; Tenne, R. *Chem. Phys. Lett.* **1994**, *227*, 235.

(6) Knobbe, E. T.; Dunn, B.; Fuqua, P. D.; Nishida, F. *Appl. Opt.* **1990**, *29*, 2729.

(7) Sorek, Y.; Zevin, M.; Reisfeld, R.; Hurvits, T.; Rushin, S. *Chem. Mater.* **1997**, *9*, 670.

(8) Zevin, M.; Reisfeld, R. *Opt. Mater.* **1997**, *8*, 37.

(9) Signorini, R.; Meneghetti, M.; Sartori, S.; Bozio, R.; Brusatin, G.; Guglielmi, M.; Maggini, M.; Scorrano, G.; Prato, M. *Non-Linear Opt.* **1998**, in press.

(10) Judeinstein, P.; Sanchez, C. *J. Mater. Chem.* **1996**, *6*, 511.

(11) Templin, M.; Wiesner, U.; Spiess, H. W. *Adv. Mater.* **1997**, *9*, 814.

(12) Peeters, M. P. J.; Wakelkamp, W. J. J.; Kentgens, A. P. M. *J. Non-Cryst. Solids* **1995**, *189*, 77.

(13) Peeters, M. P. J.; Kentgens, A. P. M. *Solid State Nucl. Magn. Res.* **1997**, *9*, 203.

(14) Lan, L.; Gnappi, G.; Montenero, A. *J. Mater. Sci.* **1993**, *28*, 2119.

(15) Hoebbel, D.; Nacken, M.; Schmidt, H. *J. Sol-Gel Sci. Technol.* **1998**, *12*, 169.

(16) Riegel, B.; Blittersdorf, S.; Kiefer, W.; Hofacker, S.; Muller, M.; Schottner, G. *J. Non-Cryst. Solids* **1998**, *226*, 76.

(17) Posset, U.; Lankers, M.; Kiefer, W.; Steins, H.; Schottner, G. *Appl. Spectrosc.* **1993**, *47*, 1600.

(18) Piana, K.; Schubert, U. *Chem. Mater.* **1994**, *6*, 1504.

(19) Philipp, G.; Schmidt, H. *J. Non-Cryst. Solids* **1986**, *82*, 31.

(20) Schmidt, H.; Seiferling, B. *Mater. Res. Soc. Symp. Proc.* **1986**, *73*, 739.

matrix represents another effect, which is not always required.

We have developed a new synthetic route to obtain GPTMS-derived sol–gel materials that is based on the epoxide ring opening by boron trifluoride diethyl etherate  $\text{BF}_3\text{O}(\text{C}_2\text{H}_5)_2$ , ( $\text{BF}_3\text{OEt}_2$ ), at room temperature. The synthesis occurs in two steps, an acid-catalyzed inorganic precondensation step, followed by the organic polymerization catalyzed by  $\text{BF}_3\text{OEt}_2$ .  $\text{BF}_3$  is a Lewis acid widely used as a catalyst of epoxide polymerization<sup>21,22</sup> whose use we have extended to sol–gel synthesis of hybrid organic–inorganic materials where the epoxy ring opening is required. In this work, we report for the first time the copolymerization of GPTMS and tetraethyl orthosilicate (TEOS), with epoxide polymerization reactions catalyzed by  $\text{BF}_3\text{OEt}_2$  at room temperature. A comparison of the effects of  $\text{BF}_3\text{OEt}_2$  with respect to other catalysts of epoxide ring opening used in sol–gel processing is reported.

### Experimental Section

**Materials.** Tetraethyl orthosilicate and (3-glycidioxypropyl)-trimethoxysilane were all analytical grade and purchased from Aldrich. Zirconium butoxide, (98%) (Aldrich), 1-methylimidazole (99%) (Aldrich), and boron trifluoride diethyl etherate (Aldrich) were used as the catalysts of epoxide polymerization. Bidistilled water for hydrolysis of alkoxides and HCl (1 N) as catalyst were used. 2,4-Pentanedione (Aldrich) was employed as chelating agent of zirconium butoxide. Methyl alcohol (Prolabo), analytical grade, was the solvent for all the sols.

Cleaned soda-lime glass microscopic slides, silica slides, and silicon wafers were used as substrates.

**Synthesis of the Precursor Sols.** The precursor sols were prepared by using a precondensation reaction, done under reflux at 80 °C for 4 h, where GPTMS and TEOS were cohydrolyzed, in acidic conditions with HCl as catalyst and methyl alcohol (MeOH) as solvent. The molar ratios between the reagents were  $\text{GPTMS}/\text{TEOS} = 7:3$  and  $(\text{GPTMS}+\text{TEOS})/\text{H}_2\text{O}/\text{HCl}/\text{MeOH} = 1:3.3:0.004:0.013$ . This buffer sol will be indicated as GT.

Three sols were prepared by adding to GT different amounts of  $\text{BF}_3\text{OEt}_2$ , with molar ratios with respect to Si of 0.01 (samples GTB01), 0.05 (samples GTB05), and 0.1 (samples GTB1). The sols were diluted by adding the proper amount of  $\text{BF}_3\text{OEt}_2$  together with methyl alcohol ( $\text{GPTMS}+\text{TEOS}/\text{MeOH} = 1:8$ ). After the addition of  $\text{BF}_3\text{OEt}_2$  the sols were left with stirring for 1 h at room temperature before using.

For comparison, with a similar procedure, other three sols were prepared, by adding to GT, as catalysts for polymerization of the epoxide groups,<sup>20,23,24</sup> 1-methylimidazole (MI) (samples GTM1) or HCl (samples GTH1) or zirconium butoxide  $\text{Zr}(\text{O}i\text{Bu})_4$  together with 2,4-pentanedione ( $\text{Zr}(\text{O}i\text{Bu})_4/2,4\text{-pentanedione} = 1:1$ ) as chelating agent (samples GTZ1). The molar ratios between the catalysts and  $\text{GPTMS}+\text{TEOS}$  were kept constant to 0.1 in all the sols. They were prepared by using two different procedures; in the first one, after the addition of the selected epoxide ring opening catalyst, the sols were left for 1 h with stirring at room temperature and then used to prepare the films. In the second one, after the catalyst addition, the sol was refluxed for 1 h at 80 °C and then used for the materials processing. These last three sols will be indicated as GTMR1, GTHR1, and GTZR1.

**Samples Preparation.** Coating films were obtained from fresh sols, by dip coating, in a humidity-controlled box, with a relative humidity below 40%. Single-layer coating films were obtained with a withdrawal speed of 120  $\text{cm min}^{-1}$ . The samples were thermally treated in air at 120 or 150 °C for 1 h. The film thickness was measured with a profilometer (Alpha Step 200, Tencor Instrument) on the step made by scratching the film after the deposition.

**Thermal Stability.** The thermal stability of the material was studied as a function of thickness and firing temperatures. Coating films with thicknesses in the range 0.5–15  $\mu\text{m}$  were directly put in the oven at different temperatures between 50 and 500 °C. The critical thickness, defined as the largest thickness free of cracks achievable after the firing treatment,<sup>25</sup> was determined.

**Infrared Spectroscopy.** Infrared absorption spectra in the range 6500–400  $\text{cm}^{-1}$  were recorded by Fourier transform infrared spectroscopy (FTIR) (Perkin-Elmer 2000) with a resolution of  $\pm 1 \text{ cm}^{-1}$ , on films deposited on silicon substrates.

**UV–Vis Spectroscopy.** UV–visible absorption spectra, in the range 190–800 nm, were taken at room temperature by a Perkin-Elmer  $\lambda$ -3B spectrophotometer, on films deposited on silica glass. The resolution was  $\pm 0.3 \text{ nm}$ .

**X-ray Diffraction Analysis.** X-ray diffraction analysis (XRD) was done on the films by a Philips PW 1740 diffractometer with a glancing angle technique.  $\text{Cu K}\alpha$ , operating at 40 kV and 50 mA, was used as the radiation source. The scan rate was 0.05° per second.

**NMR Characterization.** Nuclear magnetic resonance (NMR) spectra were recorded by a Bruker 200 AC spectrometer operating at 200.133 MHz for  $^1\text{H}$ , 50.323 MHz for  $^{13}\text{C}$ , 64.210 MHz for  $^{11}\text{B}$ , and 39.760 MHz for  $^{29}\text{Si}$ . All NMR measurements were performed in  $\text{CD}_3\text{OD}$ , used as received, by preparing the samples in 1:1 solvent/reaction mixture solutions. Peak positions were relative to tetramethylsilane and were calibrated against residual solvent resonance ( $^1\text{H}$ , 3.31 ppm) on the deuterated solvent multiplet (for  $^{13}\text{C}$ , 49.0 ppm).  $^{11}\text{B}\{^1\text{H}\}$  chemical shifts were measured relative to external  $\text{BF}_3\text{OEt}_2$ ; quantitative evaluation of the  $\text{BF}_3\text{OEt}_2$  or  $\text{H}_3\text{BO}_3$  concentrations with respect to the total amount of boron was done.  $^{29}\text{Si}$  chemical shifts were measured to external tetramethylsilane with downfield values taken as positive. Two milligrams of chromium(III) acetylacetonate was added to the samples for the  $^{29}\text{Si}$  NMR determination; pale pink solutions resulted. The relative water concentration, as a function of reaction time, was calculated by  $^1\text{H}$  NMR (s at 4.72 ppm) spectra, which were collected every 15 min of reaction of the sol.

### Results

**NMR Spectra.** The NMR spectra of GPTMS, GT, GTB1, GTM1, GTH1, and GTZ1 sols were measured. While the  $^1\text{H}$  NMR spectra were scarcely informative, the  $^{13}\text{C}$  NMR spectra gave a clear indication of the reactions occurred. Figures 1 and 2 show the  $^{13}\text{C}$  NMR spectra of GPTMS (Figures 1a and 2a), GT (Figures 1b and 2b), and GTB1 (Figures 1c and 2c). The  $^{13}\text{C}$  NMR spectra of GPTMS are characterized by the signals at 51.67 (d,  $^1J_{\text{CH}} 178.8 \text{ Hz}$ ) and 44.49 (t,  $^1J_{\text{CH}} 176.2 \text{ Hz}$ ) ppm of the CH ring and  $\text{CH}_2$  carbons, respectively<sup>26</sup> (Figure 1a). The  $\text{Si}-\text{CH}_2-\text{CH}_2$  carbons give rise to signals at 6.01 (t,  $^1J_{\text{CH}} 127.4 \text{ Hz}$ ) ppm and 23.86 (t,  $J_{\text{CH}} 116.8 \text{ Hz}$ ) ppm, respectively (Figure 2a). The  $\text{OCH}_2$  carbons appear as triplets at 74.27 ( $^1J_{\text{CH}} 141.3 \text{ Hz}$ ) and 72.66 ( $^1J_{\text{CH}} 142.9 \text{ Hz}$ ) ppm and the  $\text{OCH}_3$  groups give rise to a quartet at 50.83 ( $^1J_{\text{CH}} 142.2 \text{ Hz}$ )

(21) Kemp, D. S.; Vellaccio, F. *Organic Chemistry*; Worth Publishers Inc.: New York, 1980.

(22) Koinuma, H.; Inoue, S.; Tsuruta, T. *Die Makrom. Chemie* **1970**, *136*, 65.

(23) Popall, M.; Durand, H. *Electrochim. Acta* **1992**, *37*, 1593.

(24) Hou, L.; Mennig, M.; Schmidt, H. In *Sol–Gel Optics III*. Mackenzie, J. D., Ed. *Proc. SPIE Int. Soc. Opt. Eng.* **1994**, *2288*, 328.

(25) Innocenzi, P.; Abdirashid, M. O.; Guglielmi M. *J. Sol–Gel Sci. Technol.* **1994**, *3*, 47.

(26) Kaisemann, R.; Schmidt, H. K.; Wintruch, E. *Mater. Res. Soc. Symp. Proc.* **1994**, *346*, 915.

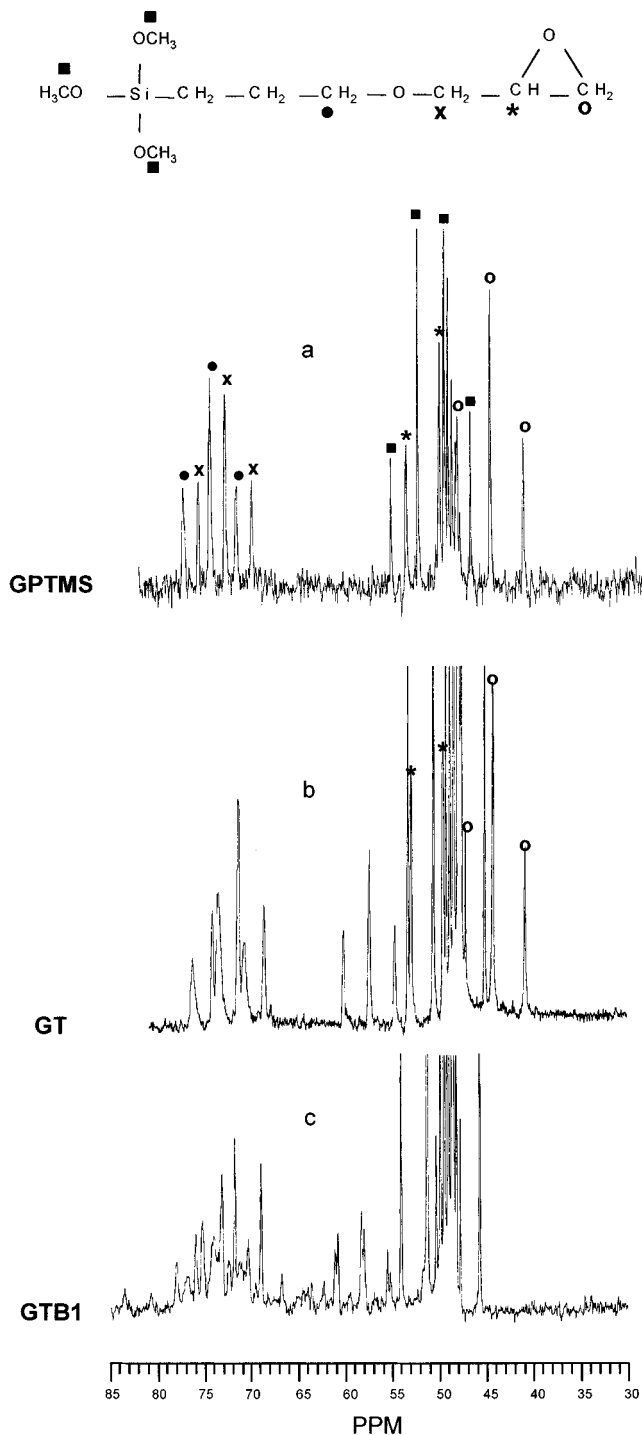


**Figure 1.**  $^{13}\text{C}$  NMR spectra of (a) GPTMS, (b) GT, and (c) GTB1 sols in the range 85–30 ppm.

ppm. The  $^{13}\text{C}$  NMR spectrum of the GT samples clearly indicates the occurrence of the hydrolysis reaction without cleavage of the epoxide rings, as shown by the maintenance of the doublet signals at 51.91 and triplet at 44.77 ppm (Figure 1b). The hydrolysis reaction produces significant modification in the Si-CH<sub>2</sub>-CH<sub>2</sub> and CH<sub>2</sub>-O-CH<sub>2</sub> patterns together with the disappearance of the -OCH<sub>3</sub> signals (Figure 1b). Because these signals are present only when the epoxy ring opening is achieved, they have been assigned to the formation of a poly(ethylene oxide) chain. The triplet around 58 ppm in Figure 1b is due to EtOH, and this attribution is confirmed by the presence of the quartet around 16

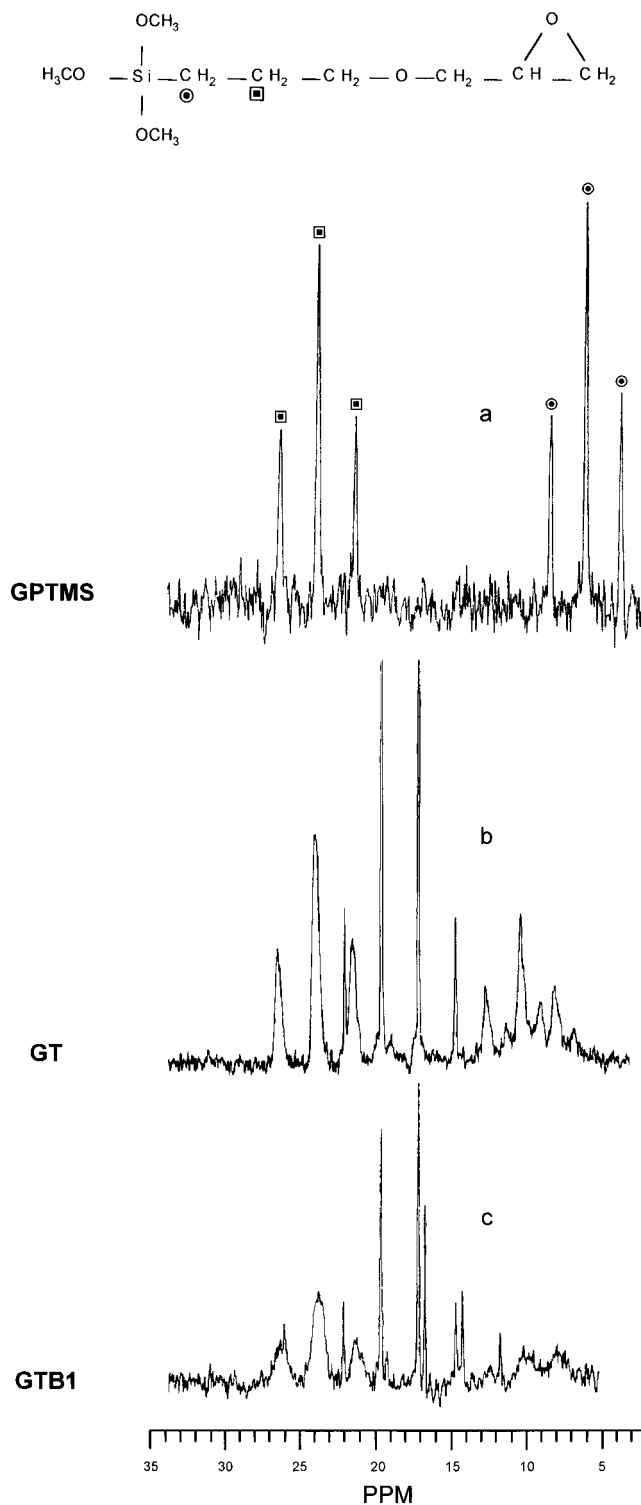


**Figure 2.**  $^{13}\text{C}$  NMR spectra of (a) GPTMS, (b) GT, and (c) GTB1 sols in the range 35–2 ppm.

ppm (Figure 2b). The EtOH was formed during the hydrolysis of TEOS. In Figure 1c, the EtOH triplet is overlapped to another triplet in the range of OCH<sub>2</sub>-CH<sub>3</sub> groups. It is noteworthy that no signal around 65 ppm is observed, thus excluding an extensive formation of diols.<sup>27</sup> The  $^{13}\text{C}$  NMR spectrum of the GTB1 sample shows the complete disappearance of the CH and CH<sub>2</sub> ring signals (Figure 1c), clearly indicating that BF<sub>3</sub>OEt<sub>2</sub>

(27) *Carbon-13 NMR Spectroscopy*; Kalinowski, H. O., Berger, S., Braun, S., John Wiley: Chichester, U.K., 1988; p 181.

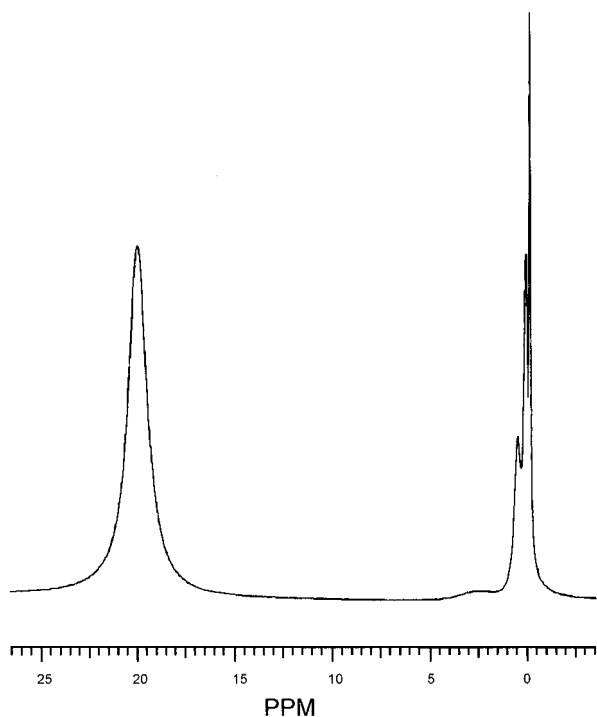


**Figure 3.**  $^{11}\text{B}$  NMR spectrum of GTB1 sol in the range 27 to  $-4$  ppm.

induced the ring opening and the subsequent formation of chains originated by epoxide polymerization. In fact, at least three new  $\text{CH}_2$  groups are well-evidenced as triplets in the NMR spectrum:  $\delta$  73.17,  $^1J_{\text{CH}}$  141.0 Hz;  $\delta$  74.04,  $^1J_{\text{CH}}$  143 Hz;  $\delta$  75.25,  $^1J_{\text{CH}}$  139.2 Hz. Additionally, there were four CH groups, appearing as broad doublets:  $\delta$  62.3,  $^1J_{\text{CH}}$  140.0 Hz;  $\delta$  68.2,  $^1J_{\text{CH}}$  140.9 Hz;  $\delta$  70.4,  $^1J_{\text{CH}}$  140.0 Hz;  $\delta$  82.2,  $^1J_{\text{CH}}$  142.7 Hz. The  $^{13}\text{C}$  NMR spectra of GTB01 and GTB05 (not shown in figures) show that 50% and 20%, respectively, of epoxide rings are still present. Finally, a comparison of the  $^{13}\text{C}$  NMR spectrum of GTB1 with those of GTM1 and GTZ1 shows that in these latter cases the signals at 51.91 and 44.77 ppm are still present, indicating the maintenance of the epoxide ring.

The  $^{11}\text{B}$  NMR spectrum of the GTB1 sample (Figure 3) shows only the presence of  $\text{BF}_3\text{OEt}_2$  at 0 ppm and boric acid as a singlet at 19.60 ppm, identified by comparison with an authentic sample. The splitting of the  $\text{BF}_3\text{OEt}_2$  signal is attributed to the different configurations of  $\text{BF}_3\text{OEt}_2$  in the sol that can be coordinated to different ethereal oxygens. No signals that could be related in the sol to the formation of mixed Si–O–B bonds were found.<sup>28</sup>

The quantitative evaluations of boron content, after the reaction, showed that  $\text{BF}_3\text{OEt}_2$  in GTB01 sols is completely transformed to  $\text{H}_3\text{BO}_3$ , while in GTB05 and GTB1, 10% and 30%, respectively, of residual  $\text{BF}_3\text{OEt}_2$  are still detected.

The  $^{29}\text{Si}$  NMR determinations were also done (Figure 4). The  $^{29}\text{Si}$  NMR spectrum of the GT samples (Figure 4b) clearly shows the occurrence of hydrolysis. In fact, the singlet of GPTMS at  $-39.52$  ppm (Figure 4a) disappears and new complex higher field signals cen-

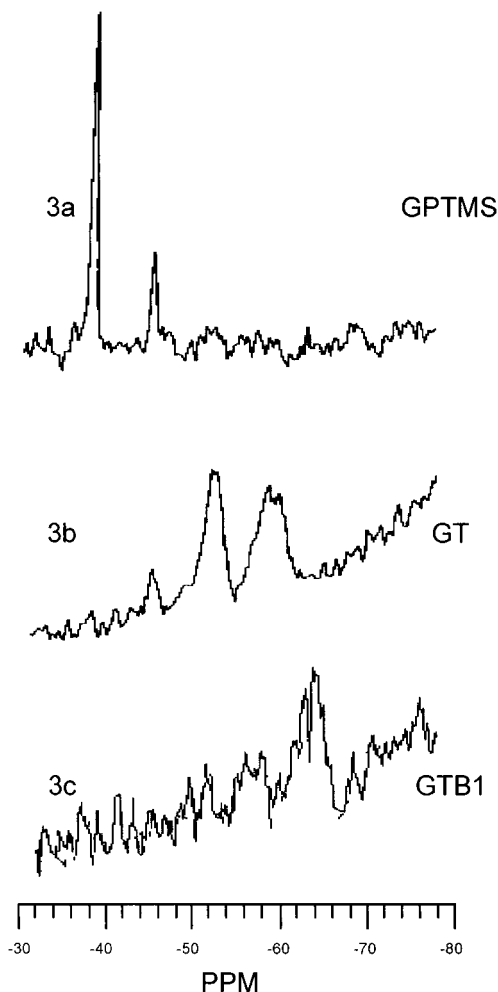


**Figure 4.**  $^{29}\text{Si}$  NMR spectra of (a) GPTMS, (b) GT, and (c) GTB1 sols in the range  $-30$  to  $-80$  ppm.

tered at  $-46.94$ ,  $-56.6$ , and  $-62.7$  ppm are present, indicating the formation of one, two, and three new siloxane bonds, respectively, from GPTMS.<sup>11,16</sup> The  $^{29}\text{Si}$  NMR spectrum of GTB1 (Figure 4c) shows the presence of a complex signal centered at  $-63.6$  ppm, due to the presence of only three siloxane bonds at this stage, which is an indication of the higher cross-linking level obtained in the presence of  $\text{BF}_3\text{OEt}_2$ .

The relative water concentration, obtained by  $^1\text{H}$  NMR spectra of GT buffer sols, exponentially decreases with the reaction time. After 240 min of reaction, the water content reaches a minimum, with a residual water that is around 50% of the starting amount. At longer reaction times no substantial decreases of water were observed.

**FTIR Spectra.** The epoxides have characteristic IR absorption bands<sup>29,30</sup> at 1260–1240 (ring breathing), 950–810 (asymmetrical ring stretching), and 865–785  $\text{cm}^{-1}$ . Another characteristic band is due to the C–H stretch in the epoxide at 3050–2995  $\text{cm}^{-1}$ . In our work, the bands peaking around 3060, 1250, and 850  $\text{cm}^{-1}$  were used as a reference for the evaluation of the epoxide polymerization in the material, together with

(29) *Comprehensive Heterocyclic Chemistry*; Lwoswski, W., Ed.; Pergamon Press: Oxford, U.K., 1984; Vol. 7, p 99.

(30) *Atlas of Spectral Data and Physical Constants for Organic Compounds*; Grasselli, J. G., Ritchey, W. M., Eds.; CRC Press Inc.: Cleveland, OH, 1975; Vol. I.

(28) Irwin, A. D.; Holmgren, J. S.; Zerda, T. W.; Jonas, J. *J. Non-Cryst. Solids* **1987**, *89*, 191.

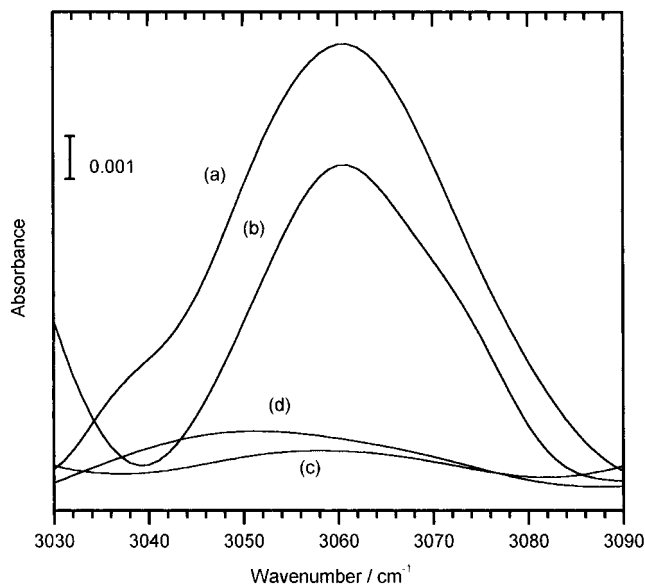


**Figure 5.** FTIR normalized spectra of GT (a), GTB01 (b), GTB05 (c), and GTB1 (d) films as deposited on silicon wafers, around  $3060\text{ cm}^{-1}$  (C–H epoxy stretch).

the absence of the diol vibration bands<sup>31</sup> at  $4080\text{ cm}^{-1}$ . Under acidic conditions, in fact, the epoxy groups may react with water to form diols that cannot further polymerize to give a poly(ethylene oxide). All the characteristic bands of epoxides are still clearly detectable in the GT as deposited films (Figure 5). The FTIR spectra of samples GTB01, GTB05, and GTB1, which contain an increasing amount of  $\text{BF}_3\text{OEt}_2$ , show a decrease in the intensity of the epoxide absorption bands with the increase of  $\text{BF}_3\text{OEt}_2$  in the precursor sols (Figure 5). The reduction in intensity of the epoxide bands with higher  $\text{BF}_3\text{OEt}_2$  contents is attributed to the epoxy ring opening catalyzed by  $\text{BF}_3\text{OEt}_2$ .

In the FTIR spectra of as deposited GTH1, GTM1, and GTZ1 films (Figure 6), the characteristic bands of epoxides are, instead, always detected. These bands do not change in intensity by thermal curing at  $120$  or  $150\text{ }^\circ\text{C}$  (not shown in the figure). GTB1 is also shown in Figure 6 for comparison.

The FTIR absorption spectra of as-deposited GTHR1, GTMR1, and GTZR1 (not reported in the figure) show that in GTHR1 and GTMR1, the epoxide bands are always clearly detected, without significant changes in intensity with respect to GTH1 and GTM1 samples, obtained from sols prepared without the additional reflux hour at  $80\text{ }^\circ\text{C}$ , after the catalyst addition. GTZ1 and GTZR1 show, instead, a different behavior, because in GTZR1 the epoxide bands are no longer observed. The thermal curing of films at  $120$  or  $150\text{ }^\circ\text{C}$  was not found to affect the epoxide bands in GTHR1 and GTMR1. In all the samples where epoxide vibrations are not detected, the characteristic absorption band of diols, around  $4800\text{ cm}^{-1}$ , was also not observed and the absence of vibrations due to the epoxide groups is assigned to epoxide polymerizations.

The FTIR spectra in Figure 7 show the decrease of  $910$  and  $855\text{ cm}^{-1}$  bands of epoxy with higher amounts of  $\text{BF}_3\text{OEt}_2$  in GTB01, GTB05, and GTB1 as deposited

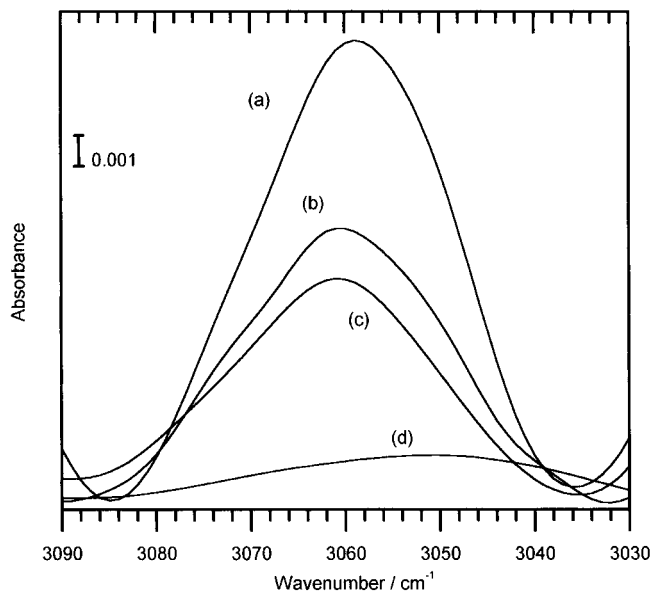


**Figure 6.** FTIR-normalized spectra of GTM1 (a), GTZ1 (b), GTH1 (c), and GTB1 (d) films as deposited on silicon wafers, around  $3060\text{ cm}^{-1}$  (C–H epoxy stretch).

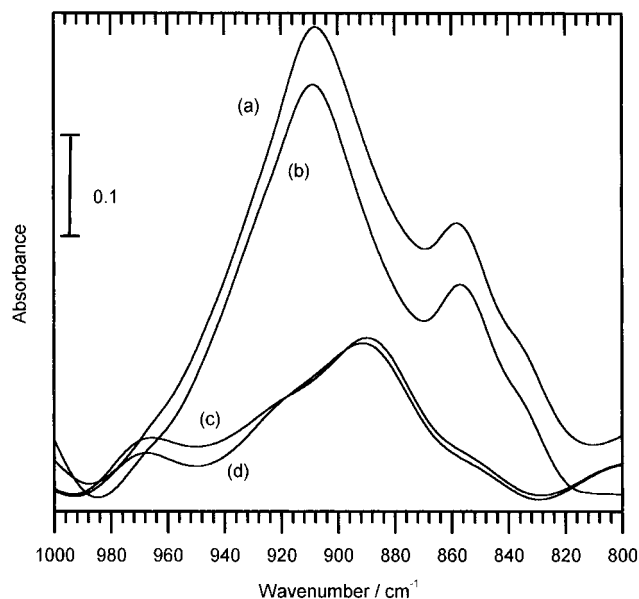


**Figure 7.** FTIR-normalized spectra of GT (a), GTB01 (b), GTB05 (c), and GTB1 (d) films as deposited on silicon wafers, around  $900\text{ cm}^{-1}$  (asymmetrical epoxy ring stretching at  $910\text{ cm}^{-1}$ , Si–O–B band at  $890\text{ cm}^{-1}$ , and epoxide band at  $850\text{ cm}^{-1}$ ).

films and the simultaneous increase of a band at  $890\text{ cm}^{-1}$ . This band is attributed to the formation of Si–O–B bonds<sup>32</sup> when higher amounts of  $\text{BF}_3\text{OEt}_2$  are used.

A strong absorption band around  $1100\text{ cm}^{-1}$ , attributed to asymmetric stretching of Si–O–Si bonds,<sup>33</sup> is observed in all the samples. This peak was found to shift to higher frequencies with the thermal treatment and to change the position as a function of the catalyst employed in the sol–gel synthesis. The exact positions of the  $1100\text{ cm}^{-1}$  band in the different samples are reported in Table 1. In all the samples, except GTB05

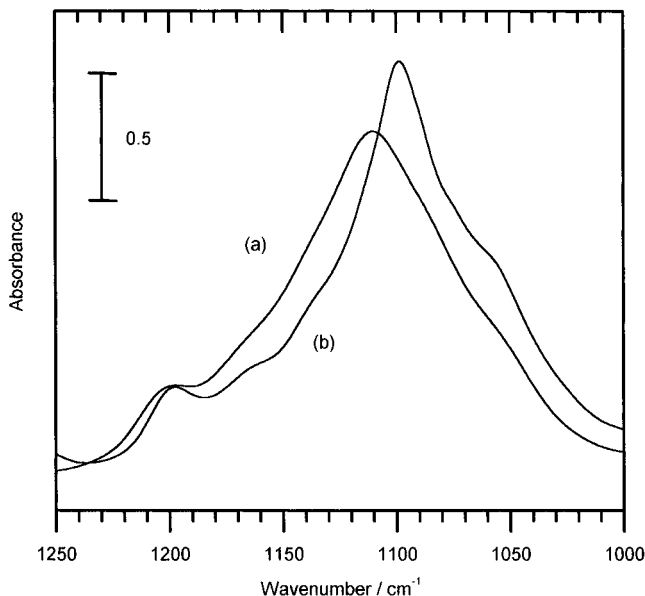
(31) Gautier-Luneau, I.; Mosset, A.; Galy, J.; Schmidt, H. *J. Mater. Sci.* **1990**, *25*, 3739.

(32) Villegas, M. A.; Navarro, J. M. *J. Mater. Sci.* **1988**, *23*, 2464.

(33) Almeida, R. M.; Pantano, C. G. *J. Appl. Phys.* **1990**, *68*, 4225.

**Table 1. Position of the Si–O–Si Band around 1100 cm<sup>-1</sup>, in the Samples Prepared by Different Epoxide-Opening Catalysts and Effect on the Epoxy Bands**

sample	as-deposited		150 °C	
	Si–O–Si band (cm <sup>-1</sup> )	epoxy bands	Si–O–Si band (cm <sup>-1</sup> )	epoxy bands
GT	1098	y	1106	y
GTB01	1101	y	1107	y
GTB05	1110	n	1110	n
GTB1	1111	n	1111	n
GTM	1103	y	1106	y
GTH	1102	y	1106	y
GTZ	1105	y	1107	y
GTMR	1111	y	1112	y
GTHR	1106	y	1108	y
GTZR	1104	n	1104	n

**Figure 8.** FTIR-normalized spectra of GTB1 (a) and GT (b) films as deposited on silicon wafers, around 1100 cm<sup>-1</sup> (asymmetrical stretching of Si–O–Si bonds).

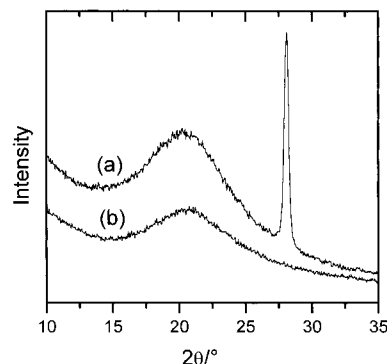
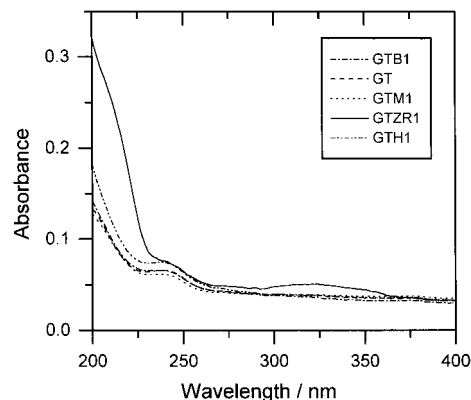
and GTB1, a shift to higher frequencies after the thermal curing is observed. In GTB05, GTB1, and GTMR1 as deposited films, the 1100 cm<sup>-1</sup> band has the highest frequency with respect to the other samples. The shift of the stretching vibration of Si–O–Si to higher frequencies is correlated to a strengthening of the network.<sup>34,35</sup>

Figure 8 shows the FTIR spectra of the region around 1100 cm<sup>-1</sup> of GT and GTB1 as deposited films. A shoulder at around 1050 cm<sup>-1</sup> is assigned to the vibrations of residual MeOH in the as deposited films.<sup>36</sup> Other three shoulders are detected in the high-frequency side of the GT spectra. Following the attribution of Viart et al.,<sup>35</sup> these shoulders are assigned as follows: the bands around 1120 and 1160 cm<sup>-1</sup> to Si–O–Si stretching vibrations of linear and less cross-linked structures, the 1200 cm<sup>-1</sup>, like the 1100 cm<sup>-1</sup> main band are, instead, due to Si–O–Si vibrations in cyclic structures. The 1200 cm<sup>-1</sup> band is overlapped to the Si–CH<sub>2</sub>

(34) Almeida, R. M.; Guitton, T. A.; Pantano, C. G. *J. Non-Cryst. Solids* **1990**, *121*, 193.

(35) Almeida, R. M.; Vasconcelos, H. C.; Ilharco, L. M. In *Sol–Gel Optics III*. Mackenzie, J. D., Ed. *Proc. SPIE Int. Soc. Opt. Eng.* **1994**, *2288*, 678.

(36) Viart, N.; Niznansky, D.; Rehspringer, J. L. *J. Sol–Gel Sci. Technol.* **1997**, *8*, 183.

**Figure 9.** XRD patterns of as-prepared GTB1 films prepared from sols with different reaction times: (a) 2 h and (b) 4 h.**Figure 10.** UV-visible absorption spectra of as deposited GT, GTB1, GTM1, GTH1, and GTZR1 films on silica glass.

wagging vibration band.<sup>30</sup> In GTB1 the shoulders attributed to vibration of Si–O–Si in linear structures are no longer observed.

**XRD Analysis.** Figure 9 shows the XRD patterns of as-deposited GTB1 films obtained from precursor sols with different reaction times. One sol was left to react 2 h under reflux at 80 °C before the addition of BF<sub>3</sub>·OEt<sub>2</sub>; in the other, the reaction time under reflux was instead extended to 4 h. The second sample, prepared from the 2 h reacted sols, showed the presence of white precipitates, which were not detected in the films deposited by the 4 h reacted sol. The XRD patterns of the films showed the presence of boric acid precipitates in the samples prepared with the 2 h reacted sols while in the films prepared from the 4 h reacted sols the H<sub>3</sub>BO<sub>3</sub> was not detected.

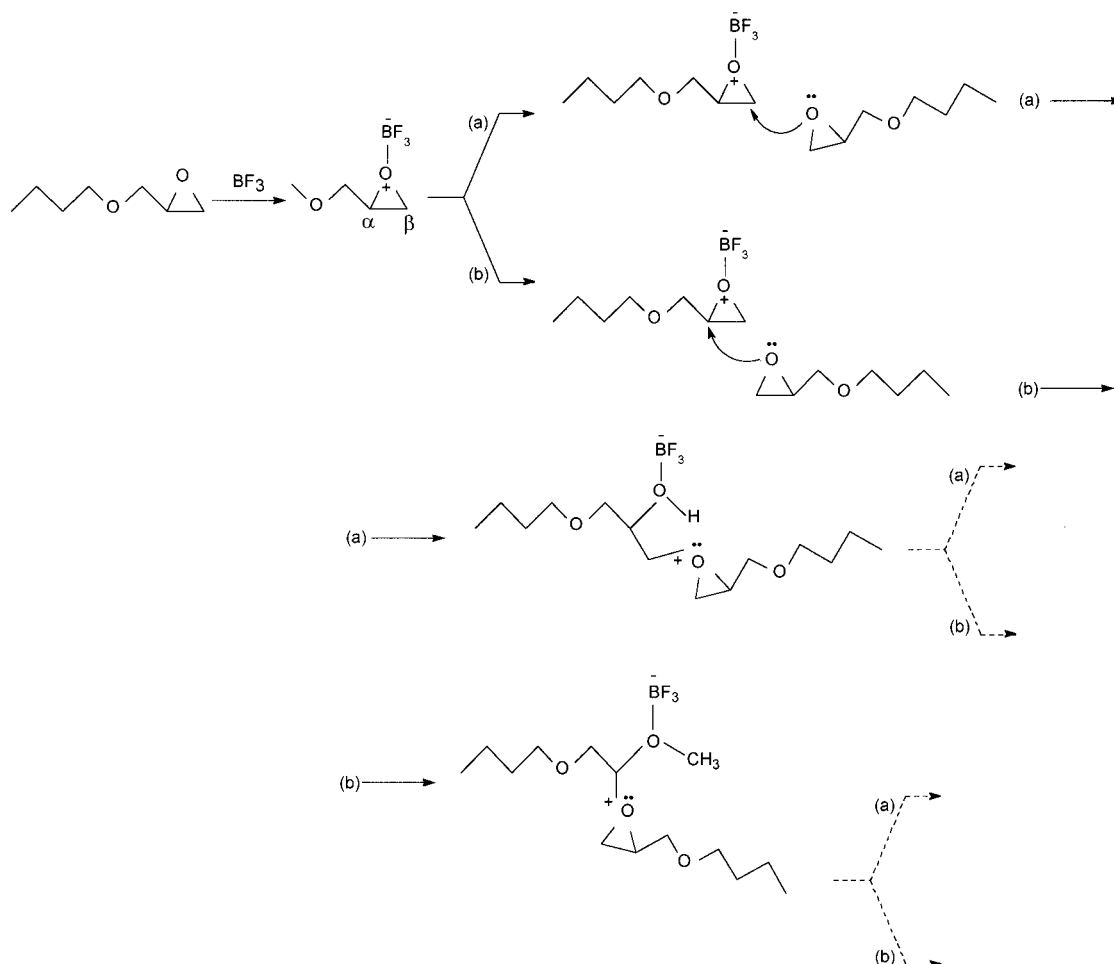
**UV-Visible Spectra.** Figure 10 shows the UV-visible absorption spectra of GT, GTB1, GTM1, GTH1, and GTZR1 films deposited on silica and fired 1 h at 150 °C. GT, GTB1, GTM1, and GTH1 have the same UV absorption edge, while in GTZR1 is shifted toward longer wavelengths. GTZR1 spectrum also shows a longer absorption tail, up to around 400 nm.

**Thermal Stability.** The samples did not crack, regardless of the thickness, up to the firing temperature of 250 °C. At 300 °C the critical thickness was around 0.9 μm, at higher treatment temperatures if the thickness did not exceed the critical one, no cracks were observed.

## Discussion

In the sol–gel processing of (3-glycidoxypropyl)tri-methoxysilane-based materials, acid or base catalysts

Scheme 1



are necessary for the hydrolysis and condensation reactions together with a specific catalyst of epoxide polymerization. The choice of this catalyst affects, however, not only the formation of the poly(ethylene oxide) chain but also the hydrolysis and condensation of GPTMS and TEOS. The NMR spectra clearly show the activity of  $\text{BF}_3\text{OEt}_2$  as catalyst for hydrolysis in agreement with the FTIR data. The  $^{13}\text{C}$  NMR spectrum of GTB1 (Figure 1) in the highfield region shows the presence of signals attributed to the  $\text{Si}-\text{CH}_2-\text{CH}_2$  groups at 8 and 24 ppm, respectively, which are significantly broader than the corresponding signals in the GT sample (Figure 2). This pattern can be explained with a worst defined magnetic environment of the Si atom as a consequence of a more extensive hydrolyzation and condensation process. Our observations are in agreement with the experiments of Templin et al.,<sup>11</sup> who found in GPTMS sols catalyzed by aluminum *sec*-butoxide a broadening of the  $\text{CH}_2$  group at 10 ppm. This effect was explained as an indirect indication of the restricted mobility of  $\text{CH}_2$  due to the large degree of condensation reached by the inorganic network. It is important to point out that the broadness increases in the order  $\text{GT} < \text{GTZ} < \text{GTM1} < \text{GTB1}$ . The same trend was observed in the FTIR spectra (Table 1), and it is confirmed by the  $^{29}\text{Si}$  experiments. All the epoxide-opening catalysts used in this work increase, with respect to GT, the degree of inorganic cross-linking. By comparing the effect of the different catalysts, however,  $\text{BF}_3\text{OEt}_2$  shows to have the highest catalytic effect on

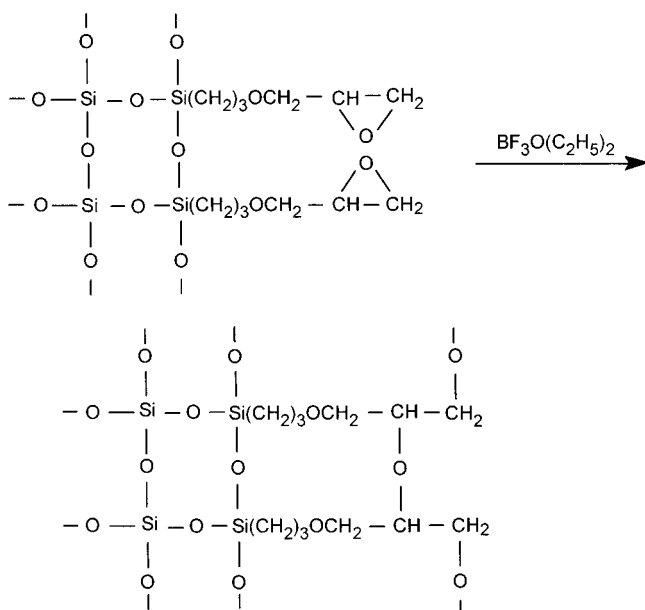
the formation of a more cross-linked inorganic network. Only MI, in GTMR1, produces on the network the same effect of  $\text{BF}_3\text{OEt}_2$ , but higher reaction times are required and do not give at the same time an efficient epoxide ring opening.

The epoxide cleavage and the formation of a poly(ethylene oxide) network is obtained at room temperature by  $\text{BF}_3\text{OEt}_2$ , as revealed by NMR of the sols and FTIR spectra of the final material. The NMR data show that  $\text{BF}_3\text{OEt}_2$  acts as catalyst in the epoxide ring opening under mild conditions.  $\text{BF}_3\text{OEt}_2$  induces polymerization with the formation of different products according to Scheme 1. In fact it is reported that alkyl-substituted oxirans can give ring opening as a consequence of both attack in  $\alpha$  (Scheme 1, route b) and  $\beta$  positions (Scheme 1, route a).<sup>37</sup> Generally, products obtained from  $\text{C}_\beta$  attack are favored, thus, in the present case we expect that products obtained through route a are preferred, involving the less hindered intermediate, too. Anyway a mixture of products is surely formed.<sup>38</sup> These facts are supported by the appearance in the  $^{13}\text{C}$  NMR spectrum of GTB1 of signals attributed to new CH and  $\text{CH}_2$  moieties while the broad triplet observed at 74.04 ppm can be attributed to the  $\text{CH}_2$  groups of polyethylene oxide systems.<sup>26</sup>

(37) (a) Eggersglus, W. *Organische Peroxyde*, Verlag Chemie: Weinheim, 1951. (b) Main, R. D.; Graupner, A. J. *Anal. Chem.* **1964**, *36*, 194. (c) Horner, L.; Jurgeleit, W. *Annalen* **1955**, *591*, 138.

(38) Edwards, J. D.; Gerrard, W.; Lappert, M. F. *J. Chem. Soc.* **1957**, 348.

Scheme 2



The use, as catalysts, of MI, HCl, or  $Zr(OBu^t)_4$  does not produce the same effect, under the same reaction conditions. Only  $Zr(OBu^t)_4$ , by using one more hour of reflux at 80 °C, after the addition to the GT sol, produces a ring opening similar to that one of  $BF_3OEt_2$ . MI allows, also, a full polymerization, but longer reaction times during the preparation are required. The use of  $BF_3OEt_2$  gives, therefore, the formation of a hybrid organic-inorganic network according to the Scheme 2.

The precondensation reaction times were found to be a very important parameter in GPTMS sols catalyzed by  $BF_3OEt_2$ . The addition of  $BF_3OEt_2$  rather than 3.5 h

of precondensation, when the water for the cohydrolysis of GPTMS and TEOS, is not completely consumed, produces precipitation of boric acid,  $H_3BO_3$ , in the material, as was observed by XRD diffraction analysis on films and NMR in the sols. Transparent materials were, instead, obtained when the residual water in the GT sol is about 50% of the starting amount.

It is important to point out that the sols with higher  $BF_3OEt_2$  concentrations, which gave transparent samples, showed the presence of  $H_3BO_3$ , as expected because of the large amount of residual water. In these films, the formation of Si-O-B bonds (Figure 6) is observed, which is an indication that, at least, some of the boron atoms become part of the inorganic network.

### Conclusions

The addition of  $BF_3OEt_2$  in a prereacted sol of GPTMS and TEOS catalyzes at room temperature the epoxide rings opening and the formation of a poly(ethylene oxide) network.  $BF_3OEt_2$  has, also, a catalytic effect on the formation of the inorganic oxide network increasing the cross-linking degree.

MI,  $Zr(OBu^t)_4$ , or HCl were found not to have the same catalytic efficiency as  $BF_3OEt_2$ . Higher reaction times or higher temperatures are generally required.

The use, as a catalyst, of  $BF_3OEt_2$  gives an alternative route to prepare GPTMS-based hybrid materials.

**Acknowledgment.** MURST, CNR (Program Materiali Innovativi (Legge 95/95)) and European Commission (DG XII) through Brite-Euram Contract BRPR-CT97-0564 are gratefully acknowledged for financial support.

CM980734Z